

1 **Introducing THOR, a model microbiome for genetic dissection of community behavior**

2

3

4 Gabriel L. Lozano^{1,2}, Juan I. Bravo^{1,2}, Manuel F. Garavito Diago¹, Hyun Bong Park^{3,4}, Amanda
5 Hurley¹, S. Brook Peterson⁵, Eric V. Stabb⁶, Jason M. Crawford^{3,4,7}, Nichole A. Broderick⁸, Jo
6 Handelsman^{1,2*}

7

8

9 ¹Wisconsin Institute for Discovery and Department of Plant Pathology, University of Wisconsin-
10 Madison

11 ²Department of Molecular, Cellular and Developmental Biology, Yale University

12 ³Department of Chemistry, Yale University

13 ⁴Chemical Biology Institute, Yale University

14 ⁵Department of Microbiology, University of Washington

15 ⁶Department of Microbiology, University of Georgia

16 ⁷Department of Microbial Pathogenesis, Yale School of Medicine

17 ⁸Department of Molecular and Cell Biology, University of Connecticut

18

19 *To whom correspondence should be addressed jo.handelsman@wisc.edu

20

21

22

23 **ABSTRACT**

24 The quest to manipulate microbiomes has intensified, but many microbial communities have
25 proven recalcitrant to sustained change. Developing model communities amenable to genetic
26 dissection will underpin successful strategies for shaping microbiomes by advancing
27 understanding of community interactions. We developed a model community with
28 representatives from three dominant rhizosphere taxa: the Firmicutes, Proteobacteria, and
29 Bacteroidetes. We chose *Bacillus cereus* as a model rhizosphere Firmicute and characterized
30 twenty other candidates, including “hitchhikers” that co-isolated with *B. cereus* from the
31 rhizosphere. Pairwise analysis produced a hierarchical interstrain-competition network. We
32 chose two hitchhikers — *Pseudomonas koreensis* from the top tier of the competition network
33 and *Flavobacterium johnsoniae* from the bottom of the network to represent the Proteobacteria
34 and Bacteroidetes, respectively. The model community has several emergent properties—
35 induction of dendritic expansion of *B. cereus* colonies by either of the other members and
36 production of more robust biofilms by the three members together than individually. Moreover,
37 *P. koreensis* produces a novel family of alkaloid antibiotics that inhibit growth of *F. johnsoniae*,
38 and production is inhibited by *B. cereus*. We designate this community THOR, because the
39 members are *the hitchhikers of the rhizosphere*. The genetic, genomic, and biochemical tools
40 available for dissection of THOR provide the means to achieve a new level of understanding of
41 microbial community behavior.

42

43 **IMPORTANCE**

44 The manipulation and engineering of microbiomes could lead to improved human health,
45 environmental sustainability, and agricultural productivity. However, microbiomes have proven

46 difficult to alter in predictable ways and their emergent properties are poorly understood. The
47 history of biology has demonstrated the power of model systems to understand complex
48 problems such as gene expression or development. Therefore, a defined and genetically tractable
49 model community would be useful to dissect microbiome assembly, maintenance, and processes.
50 We have developed a tractable model rhizosphere microbiome, designated THOR, containing
51 *Pseudomonas koreensis*, *Flavobacterium johnsoniae*, and *Bacillus cereus*, which represent three
52 dominant phyla in the rhizosphere, as well as in soil and the mammalian gut. The model
53 community demonstrates emergent properties and the members are amenable to genetic
54 dissection. We propose that THOR will be a useful model for investigations of community-level
55 interactions.

56

57 **KEYWORDS**

58 model community, rhizosphere, *Bacillus cereus*, *Pseudomonas koreensis*, *Flavobacterium*
59 *johnsoniae*, inhibitory network, biofilm, colony expansion, emergent properties.

60

61 INTRODUCTION

62 Modern understanding of microbiomes has been accompanied by recognition of their vast
63 complexity, which complicates their study and manipulation. Powerful –omics approaches that
64 profile community features such as genomes, metabolites, and transcripts have illuminated the
65 richness of many communities (1). These global portraits of complex communities have been
66 complemented by genetic and biochemical dissection of much simpler communities and, in
67 particular, binary interactions of one bacterial species with one host such as bacterial symbionts
68 of legume roots (2) and squid light organs (3). Study of these systems has elucidated the
69 pathways regulating interactions among bacteria and between bacteria and their environments.

70 The explosion of understanding of two-species interactions has generated a scientific
71 thirst for more tools to attain mechanistic understanding of multi-species community behaviors.
72 Model systems consisting of more than one microbial member include communities in flies (4,
73 5), the medicinal leech (6), and engineered systems (7). Key among the traits that demand more
74 mechanistic studies are the components of community assembly and robustness, which is the
75 ability to resist and recover from change (8, 9). Understanding these traits has particular value
76 today as many researchers aim to modify microbial communities to achieve outcomes to improve
77 human health, environmental sustainability, and agricultural productivity.

78 Over the last century, the challenge to alter microbial communities in predictable ways
79 has stymied microbiologists. Examples include attempts to change the human gut microbiome by
80 ingestion of yogurt or probiotics (10) or to alter plant microbiomes with inundative application of
81 disease-suppressive microorganisms (11). Few treatments have induced long-term changes due
82 to intrinsic community robustness.

83 Communities express emergent properties, which are traits that cannot be predicted from
84 the individual members (12). For example, metabolic exchange between yeast and *Acetobacter*
85 yields a mixture of volatile compounds attractive to *Drosophila* hosts that was not produced by
86 either microbe in pure culture (13). Such higher-order or emergent properties of communities
87 (14) might explain the difficulty in manipulating them. In addition, many communities contain
88 functional redundancy that is likely to contribute to robustness.

89 Classical genetic analysis, defined as the isolation and study of mutants, in model
90 organisms has advanced understanding of processes such as gene regulation in *E. coli* and the
91 mouse, and development in flies and nematodes, but such reductionist genetic approaches are
92 inaccessible in most microbial community-level analyses. A genetically tractable model system
93 for studying microbial community assembly and robustness has the potential to transform our
94 understanding of community processes. The scientific community recognizes the power of model
95 systems in relation to microbial communities (15-17) and many groups have started to address
96 this call (18-20). Importantly, common microbiome principles will only emerge with a diverse
97 set of models to interrogate. Toward this end we developed a model system involving three
98 bacterial species—*Pseudomonas koreensis*, *Flavobacterium johnsoniae*, and *Bacillus cereus*—
99 which interact under field and laboratory conditions, are amenable to genetic analysis, and
100 represent three major phyla in microbiomes on plant roots and in the human gut.

101

102 **RESULTS**

103 **Source of community members.** We sought a model community that is simple and
104 contains genetically tractable species that likely interact under natural conditions, both
105 competitively and cooperatively. We drew upon our previous work demonstrating the peculiar

106 tendency of *B. cereus* to carry “hitchhikers” (21) when it is isolated from soybean roots. These
107 biological hitchhikers are cryptic bacteria that become visible in culture only after apparently
108 pure cultures of *B. cereus* are maintained at 4°C for several weeks (22). It is important to note
109 that biological hitchhiking involves a physical association and is distinct from genetic
110 hitchhiking which selects for neutral alleles (23). Most hitchhikers are members of the
111 Bacteroidetes phylum with a small proportion from the Proteobacteria and Actinomycetes (22).
112 We selected twenty-one candidates that include *B. cereus* UW85, twelve hitchhikers, and eight
113 other isolates from the roots that harbored the hitchhikers (Fig. 1B-C). These isolates represented
114 the four dominant phyla present in the rhizosphere: Firmicutes, Proteobacteria, Bacteroidetes,
115 and Actinobacteria (24).

116

117 **High-order organization structures in an inhibitory interaction network of**
118 **rhizosphere isolates.** Competition plays an important role in microbial communities (25). To
119 identify competitive interference interactions in our collection of twenty-one rhizosphere
120 isolates, we evaluated them in pairs for inhibition of the other members in three different media.
121 Of 105 inhibitory interactions detected, 71 (68%) were conserved in at least two growth
122 conditions and 27 were conserved in all three conditions (Fig. 1A). From the 105 inhibitory
123 interactions observed among the rhizosphere bacteria, we constructed a matrix (Fig. 1C). The
124 strains display a high degree of interaction, indicated by high connectance (value of $C = 0.24$,
125 which represents the fraction of all possible interactions or $\# \text{ interactions} / \# \text{ species}^2$). On
126 average, each isolate interacted with six other isolates, as either the source or target of inhibition.
127 The interaction matrix appears to be producer determined with a negative sender-receiver
128 asymmetry value of $(Q) = -0.31$ (26). This suggests that the structure of the inhibitory networks

129 is more controlled by the producers and their secreted antibiotics than by the tester strains.
130 Connectance values reported previously for diverse food-web structures are between 0.026 and
131 0.315 (27), and the strains tested in this study had a value of 0.24, indicating high connectance.

132 To detect higher order community organization mediated by inhibitory interactions, we
133 used a hierarchy-scoring scheme in which the ability to inhibit was given a positive score and
134 sensitivity generated a negative score (Fig. 1D). We observed inhibitory hierarchical interactions
135 in which the top isolates of the network inhibit isolates that receive a medium score, and in turn
136 these medium-scoring isolates inhibit isolates that receive a lower score (Fig. 1E-F).

137 The four isolates that received the highest score, *Delftia acidovorans* and three
138 *Pseudomonas* spp., were responsible for 58 (55%) of the inhibitory interactions (Fig. 1E). Non-
139 hierarchical interactions were infrequent (6%), and these were largely reciprocal interactions
140 between six isolates with middle and low scores, such as *Lysobacter* sp. RI17 (Fig. 1G), which is
141 inhibited by five isolates under almost all conditions. Reciprocal inhibition by *Lysobacter* sp.
142 against these strains appeared predominantly in the lower nutrient condition (1/10th-strength
143 TSA).

144

145 ***P. koreensis* isolate inhibits members of the Bacteroidetes in root exudate.** Three of
146 the strains inhibited most of the other isolates, placing them at the top of the inhibitory network.
147 These strains were all members of the *P. fluorescens* complex. They are the only members of the
148 collection that consistently inhibit *Bacteroidetes* isolates, which is the most abundant phylum
149 among the co-isolates of *B. cereus*, making the inhibitory activities of these *P. fluorescens*
150 members of particular interest. In addition, members of the *P. fluorescens* group have been
151 shown to alter the structure of microbial communities on roots, making the inhibition of

152 Bacteroidetes of interest to understand communities (28). To determine whether the three
153 *Pseudomonas* strains inhibit members of the *Bacteroidetes* similarly, we tested them against *F.*
154 *johnsoniae* CI04. *Pseudomonas* sp. CI14 and *Pseudomonas* sp. RI46 inhibited *F. johnsoniae*
155 CI04 growth in standard media and *P. koreensis* CI12 inhibited *F. johnsoniae* CI04 only in root
156 exudate (Fig. 2A). Against a panel of diverse rhizosphere isolates grown in root exudate, *P.*
157 *koreensis* CI12 inhibited primarily Bacteroidetes strains (Fig. 2B).

158

159 ***B. cereus* protects *F. johnsoniae* from *P. koreensis* by modulating levels of**
160 **koreenceine metabolites.** To explore the ecology of *B. cereus* and its hitchhikers, *P. koreensis*
161 CI12 and *F. johnsoniae* CI04, we added *B. cereus* UW85 to the co-culture of the hitchhikers.
162 Unpredictably, *B. cereus* UW85 enabled growth of *F. johnsoniae* CI04 in co-culture with *P.*
163 *koreensis* CI12 (Fig. 2C) without affecting growth of *P. koreensis* CI12 (Fig. S1). *F. johnsoniae*
164 protection is dependent upon *B. cereus* arrival at stationary phase (Fig. S2). *B. subtilis*
165 NCIB3160, a well-studied spore-forming bacterium, also protected *F. johnsoniae* in a stationary
166 phase-dependent manner (Fig. S2). Among three *B. subtilis* NCIB3160 mutants affected in
167 transcriptional regulators related to stationary phase (29), only the mutant affected in *spo0H*,
168 which controls the early transition from exponential to stationary phase, was unable to protect *F.*
169 *johnsoniae* from *P. koreensis* (Fig. 3). A *spo0H* mutant in *B. cereus* UW85 also did not protect
170 *F. johnsoniae* from *P. koreensis* (Fig. 3).

171 We recently described a *P. koreensis* family of bacterial alkaloids—koreenceine A, B,
172 and C—that influence growth of *F. johnsoniae* in root exudates (30). Cell-free filtrates of co-
173 cultures of *P. koreensis* and *F. johnsoniae* inhibit *F. johnsoniae* growth, whereas filtrates of *P.*
174 *koreensis* cultured alone or with both *F. johnsoniae* and *B. cereus* do not inhibit *F. johnsoniae*

175 growth (Table 1). The levels of koreenceine A, B, and C were higher when *P. koreensis* was co-
176 cultured with *F. johnsoniae* than when it was cultured alone (Table 1). Addition of *B. cereus* to
177 co-cultures of *P. koreensis* and *F. johnsoniae* severely reduced accumulation of koreenceine A
178 and C with a minor effect on the level of koreenceine B. The *B. cereus* $\Delta spo0H$ mutant did not
179 protect *F. johnsoniae* in triple culture, nor did it reduce accumulation of koreenceine A and C as
180 substantially as did wild type *B. cereus* (Table 1). We propose that *B. cereus* protects *F.*
181 *johnsoniae* by selectively reducing the levels of koreenceine A and C accumulated by *P.*
182 *koreensis*.

183

184 **Rhizosphere isolates modulate *B. cereus* colony expansion.** Among twenty rhizosphere
185 isolates, six induced *B. cereus* patches to expand in a dendritic pattern when plated on a lawn of
186 the corresponding isolate on $1/10^{\text{th}}$ -strength TSA (Fig. 4). *B. cereus* was the only isolate of the
187 collection that displayed colony expansion. A similar motility pattern has been observed in *B.*
188 *cereus* translocating in an artificial soil microcosm (31), suggesting that this motility might be
189 important in adapting to the soil environment. In pure culture, *B. cereus* colonies expanded in an
190 irregular pattern with dense branches and asymmetrical bulges, whereas on lawns of the six
191 isolates, including *P. koreensis* and *F. johnsoniae*, expansion was greater and radially
192 symmetrical (Fig. 4, Fig. 5A, Table S1). Colonies of *B. cereus* spread into the neighboring
193 colonies of *F. johnsoniae* CI04 and *P. koreensis* CI12 when the two strains were grown in close
194 proximity on plates (Fig. 5B). *B. cereus* spread both around and across *P. koreensis* CI12, and
195 across, but not around, *F. johnsoniae* CI04. *B. cereus* did not display colony expansion when in
196 contact with or proximal to *Paenibacillus* sp. RI40 (Fig. 5).

197

198 **Rhizosphere isolates modulate *Pseudomonas* biofilm formation.** Among the
199 hitchhikers and rhizosphere isolates, *Pseudomonads spp.* isolates produced the most robust
200 biofilms (Fig. 6A). In pairwise tests, poor biofilm producers changed the behavior of isolates of
201 *Pseudomonas spp.* (Fig. 6B-D). When alone, *P. koreensis* CI12 produced maximum biofilm at
202 18 h, after which the biofilm began to dissociate (Fig. S3). *F. johnsoniae* CI04 and *B. cereus*
203 UW85 each increased the maximum biofilm formed by *P. koreensis* CI12 at 18 h, and reduced
204 the rate of biofilm dissociation (Figure 6E-F). A mixture of all three strains followed the same
205 pattern as the pairs, although the triple mixture maintained more biofilm at 36 hours ($p < 0.01$)
206 (Fig. 6F), suggesting that *F. johnsoniae* CI04 and *B. cereus* UW85 together sustain the *P.*
207 *koreensis* CI12 biofilm longer than either alone.

208

209 **DISCUSSION**

210 We constructed a model community built upon microbes isolated from the soybean
211 rhizosphere. We selected *B. cereus* as the first member of the community because of its
212 ubiquitous distribution in soil and on roots (32) and its influence on the rhizosphere (33-36).
213 Approximately 3 to 5% of *B. cereus* colonies isolated from roots carry “hitchhikers”—other
214 species that are only visible in culture over time in cold storage (22). *B. cereus* and its
215 hitchhikers are derived from the same habitat and appear to have a physically intimate
216 association, suggesting that their interactions in culture are relevant to the natural community;
217 therefore, the second and third candidates for the model community were chosen from among the
218 hitchhikers.

219 The second candidate was *F. johnsoniae*, a member of the Bacteroidetes, the most
220 abundant group of hitchhikers. *B. cereus* enables *F. johnsoniae* to grow in soybean and alfalfa

221 root exudate by providing fragments of peptidoglycan as a carbon source (22). The third
222 candidate for the model community was *P. koreensis*, which inhibits growth of *F. johnsoniae* in
223 soybean root exudates, but not when *B. cereus* is present. Other interactions among these three
224 species include modulation of *B. cereus* colony expansion by *F. johnsoniae* and *P. koreensis* and
225 enhancement of *P. koreensis* biofilm formation by *B. cereus* and *F. johnsoniae*. These three
226 candidates are genetically tractable, their genomes have been sequenced (21, 37, 38), they
227 represent three phyla that dominate the rhizosphere and other host-associated communities (39-
228 44), and they display both competitive and cooperative interactions. We designate the model
229 community containing *B. cereus*, *F. johnsoniae*, and *P. koreensis* as “THOR,” to indicate the
230 members are *the hitchhikers of the rhizosphere*.

231 THOR has two emergent properties, colony expansion and biofilm formation, that are
232 increased by the complete community and could not be predicted from the behavior of the
233 individuals. Each are observed with several combinations of community members,
234 demonstrating functional redundancy in the system. *B. cereus* colony expansion likely reflects
235 other bacteria affecting *B. cereus* motility. To our knowledge, this is the first report to indicate *B.*
236 *cereus* motility influenced by social interactions. Motility influenced by social interactions is a
237 rapidly growing field of research that has already demonstrated diverse mechanisms by which
238 bacteria modulate motility in other species, including diffusible metabolites and cell-to-cell
239 contact (45, 46). The *B. cereus* dendritic growth patterns described here have been associated
240 with sliding motility in semi-solid agar under low-nutrient conditions (47), and in artificial soil
241 microcosms (31). Sliding is a passive appendage-independent translocation mechanism mediated
242 by expansive forces of a growing colony accelerated by biosurfactants (48). Future experiments

243 will determine whether *B. cereus* colony expansion over a bacterial lawn is mediated by sliding
244 and whether the inducing bacteria enable this motility with biosurfactants.

245 Biofilm produced by *P. koreensis* CI12 was augmented and sustained by other THOR
246 members. *P. koreensis* CI12 is a member of the *P. fluorescens* complex, which contains many
247 members that promote growth and suppress disease of plants, processes often dependent upon
248 biofilm formation (49). The community modulation of *P. koreensis* CI12 biofilm formation and
249 persistence could be a strategy to maintain bacteria in the rhizosphere. The social interactions
250 among the members of the THOR model community provides an experimental system to probe
251 mechanisms of *P. koreensis* biofilm assembly and disassembly and its role in *P. koreensis*
252 lifestyle within a rhizosphere community.

253 In addition to having emergent community properties, THOR members interact in several
254 ways that are common in communities. *B. cereus* increases *F. johnsoniae* growth through
255 nutritional enhancement (22) and protects it from growth inhibition by *P. koreensis*, illustrating
256 how pairwise interactions can be modulated by other members of the community, a phenomenon
257 observed previously in synthetic communities (50, 51). Growth interference and enhancement
258 have been considered rare in naturally occurring communities because these behaviors often
259 cannot be predicted from pairwise interactions (52). Our results further reinforce the importance
260 of community modulation of behaviors observed in pairwise studies.

261 THOR was constructed from a collection of 21 rhizosphere isolates that share several
262 properties such as high interactivity and high-order organization mediated by antagonistic
263 interactions with previously proposed model communities (26, 53, 54). We show that these
264 properties can originate from phylogenetically diverse bacteria. We propose that the high

265 microbial diversity detected in soil and rhizosphere communities could be in part achieved by
266 hierarchical inhibition coupled with modulation of inhibition.

267 A genetically tractable community with defined composition in a controlled environment
268 offers the opportunity to dissect the mechanisms by which communities are established, function,
269 and maintain their integrity in the face of perturbation. Rigorous testing of the numerous
270 mechanistic hypotheses about community behavior that have been generated by -omics analyses
271 requires systems in which variables can be isolated. This is offered in genetically tractable
272 systems in which the functions of individual genes can be established through mutant analysis,
273 and the impact of environmental factors can be studied by manipulating each variable. Therefore,
274 model systems that can be fully dissected need to be part of the arsenal of tools to advance
275 microbial ecology to a new platform of experimental power and causal inference.

276 We present THOR as a simple, multi-phylum, genetically tractable system with diverse
277 community characteristics, some of which are the result of emergent properties. To capture the
278 impact of multi-organism interactions and emergent properties, communities need to be studied
279 as single genetic entities. Metagenomics introduced the concept of the community as the unit of
280 study for genomes; similarly, “metagenetic” analysis will apply genetic analysis at the
281 community level for mechanistic understanding (55). Such understanding will be key to
282 designing interventions to achieve outcomes in the health of humans, the environment, and the
283 agroecosystem.

284

285 **ACKNOWLEDGMENTS**

286 We gratefully acknowledge Jennifer Heinritz for her assistance with microscopy. This research
287 was supported by the Office of the Provost at Yale University, by funding from the Wisconsin

288 Alumni Research Foundation through the University of Wisconsin–Madison Office of the Vice
289 Chancellor for Research and Graduate Education, and by NSF grant MCB-1243671.

290

291 **MATERIALS AND METHODS**

292

293 **Bacterial strains and culture conditions.** *B. cereus* UW85 and 20 co-isolates and
294 rhizosphere isolates were reported previously (22)(Table S2). *B. subtilis* NCIB3160 WT, *spo0A*,
295 *spo0H* and *sigF* were a gift from Roberto Kolter at Harvard University. Bacterial strains were
296 propagated on 1/10th-strength tryptic soy agar (TSA) and grown in liquid culture in 1/2-strength
297 tryptic soy broth (TSB) at 28°C with vigorous shaking. *Bacillus* spores were quantified by
298 plating on 1/10th TSA after heating at 80°C for 10 min.

299

300 **Production of root exudates.** Soybean seeds were surface disinfected with 6% sodium
301 hypochlorite for 10 min, washed with sterilized deionized water, transferred to water agar plates,
302 and allowed to germinate for three days in the dark at 25°C. Seedlings were grown in a
303 hydroponic system using modified Hoagland's plant growth solution (56). Root exudate was
304 collected after 10 days of plant growth in a chamber (12-h photoperiod, 25°C), filter sterilized
305 and stored at -20°C. An amino acid mix of equal parts alanine, aspartate, leucine, serine,
306 threonine, and valine was added to the root exudate at a final concentration of 6 mM.

307

308 **Generating an inhibitory interaction network between rhizosphere bacteria.** The
309 presence or absence of inhibitory interactions between strains in our collection was evaluated
310 following a modified spread-patch method. Strains were grown individually for 20 h. One-mL

311 aliquots of cultures of each strain were centrifuged ($6000 \times g$, 6 min), resuspended in 1 ml of the
312 same medium (undiluted cultures), and a 1:100 dilution of each strain was prepared in the same
313 medium (diluted culture). Inhibitory interactions were evaluated in three different media plates:
314 Luria-Bertani agar, 1/2-strength TSA, and $1/10^{\text{th}}$ -strength TSA. Plates were spread with 100 μL
315 of the diluted cultures and spotted with 10 μL of the undiluted cultures, with four strains per
316 plate. Plates were then incubated at 28°C and inspected for zones of inhibition after two days. A
317 network of inhibitory interactions was then generated using the inhibitory interaction matrix that
318 summarize the detected interactions in the three conditions evaluated, where each node of the
319 network represents one of the bacterial strains and each edge represents growth inhibition of the
320 target. A simple hierarchy scoring was created to assign hierarchy levels based on Wright &
321 Vetsigian, 2016 (54). Each strain was assigned one “reward” point for inhibiting another strain
322 and one “penalty” point for each strain that inhibited it. One penalty point was also assigned for
323 reciprocal interactions. Networks were visualized using Cytoscape software (57). The sender-
324 receiver asymmetry (Q) was calculated from the inhibitory interaction matrix as reported by
325 Vetsigian et al., 2011 (26).

326

327 **Competition assays in liquid culture.** Strains were grown individually for 16 to 20 h. A
328 one-mL sample was removed from each overnight culture and the cells were washed once and
329 resuspended in phosphate-buffered saline (PBS). Culture medium was inoculated with $\sim 10^6$ *F.*
330 *johnsoniae* cells mL^{-1} , and $\sim 10^7$ *Pseudomonas* cells mL^{-1} . *B. cereus* and *B. subtilis* were
331 inoculated at densities between $\sim 10^4$ cells mL^{-1} to $\sim 10^7$ cells mL^{-1} , depending upon the
332 experiment. When evaluating the susceptibility of each strain to *P. koreensis* CI12 inhibition in

333 root exudate, all strains except CI12 were inoculated at a final density of 1/1000 their overnight
334 culture density. Cultures were incubated with agitation for two days at 28°C. Samples were
335 withdrawn periodically to evaluate bacterial growth by serial dilution and plating. The initial
336 densities were determined on either LB or LB containing kanamycin (10 $\mu\text{g mL}^{-1}$). At every
337 other time point, *Pseudomonas* sp. colonies were counted on LB plates, *Bacillus* sp. were
338 selected on LB plates containing polymyxin B (4 $\mu\text{g mL}^{-1}$), and all other strains were selected on
339 LB plates containing kanamycin (10 $\mu\text{g mL}^{-1}$). Plates were incubated at 28°C for two days.

340

341 **Chromosomal deletion of *spo0H* in *B. cereus*.** The gene encoding the Spo0H sigma
342 factor was deleted using a chromosomal integration vector with a thermosensitive origin of
343 replication that introduces the deletion with no marker. Construction of the *spo0H* deletion
344 cassette was accomplished by a modified version of overlap extension (OE) PCR strategy.
345 Fragments one kb upstream and one kb downstream of the *spo0H* gene were amplified using
346 primers mut_spo0HA1/mut_spo0HA2 and mut_spo0HB1/mut_spo0HB2 respectively (Table
347 S3). The PCR products were cloned in pENTR/D-TOPO, generating pmut_spo0H_ENTR.
348 Primers mut_spo0HA1 and mut_spo0HB2 were designed to include a BamHI site in the 5'
349 region to allow transfer. The *spo0H* deletion construct was recovered from pmut_spo0H_ENTR
350 using BamHI, and cloned in the BamHI site of pMAD, generating pmut_spo0H_MAD in *E. coli*
351 GM2929. Gene replacement was carried out in a manner similar to the method described
352 previously (58). Briefly, pmut_spo0H_MAD was introduced into *B. cereus* UW85 by
353 electroporation in 0.2-cm cuvettes with a Gene Pulser (BioRad Laboratories) set at 1.2 kV. The
354 surviving cells were cultured on 1/2-strength TSA plates with erythromycin (3 $\mu\text{g mL}^{-1}$) and X-

355 Gal ($50 \mu\text{g mL}^{-1}$) at 28°C . Strains that had undergone the single recombination event were
356 selected on plates containing erythromycin ($3 \mu\text{g mL}^{-1}$) at 40.5°C . To select for a second
357 crossover event, single recombinant clones were grown at 28°C in nonselective media, diluted
358 into fresh medium and then grown at 40.5°C , and plated for single colonies on 1/2-strength TSA
359 with X-Gal ($50 \mu\text{g mL}^{-1}$) at 40.5°C . White colonies, which were putative double recombinants,
360 were confirmed by PCR using mut_spo0HA1 and mut_spo0HB2 for the deletion of *spo0H*.

361
362 **Identification of koreenceine metabolites produced by *P. koreensis* CI12 in the**
363 **presence of other rhizosphere members.** *P. koreensis* CI12 was grown alone, in co-culture or
364 in triple culture with other rhizosphere members in root exudate at 28°C with agitation. Five mL
365 of cultures were centrifuged ($6000 \times g$, 6 min), and supernatants were filtered using a $0.22\text{-}\mu\text{m}$
366 pore size polyethersulfone (PES) membrane filter (Millipore). The cell-free cultures were mixed
367 with 6 mL of 2-butanol. Six mL of the organic phase was concentrated using a GeneVac EZ-2
368 plus (SP Scientific). Crude extracts were resuspended in methanol and analyzed on an Agilent
369 6120 single quadrupole liquid chromatography-mass spectrometry (LC/MS) system (Column:
370 Phenomenex kinetex C_{18} column, $250 \times 4.6 \text{ mm}$, $5 \mu\text{m}$; flow rate: 0.7 mL min^{-1} ; mobile phase
371 composition: H_2O and acetonitrile (ACN) containing 0.1% trifluoroacetic acid (TFA); method:
372 0-30 min, 10-100% ACN; hold for 5 min, 100% ACN; 1 min, 100-10% ACN). High-resolution
373 electrospray ionization mass spectrometry (HR-ESIMS) data were obtained using an Agilent
374 iFunnel 6550 Q-TOF (quadrupole-time-of-flight) mass spectrometer fitted with an electrospray
375 ionization (ESI) source coupled to an Agilent (USA) 1290 Infinity high performance liquid
376 chromatography (HPLC) system.

377 ***B. cereus* motility assay.** *B. cereus* motility was evaluated using the same modified
378 spread-patch method described above. We used *B. cereus* UW85/pAD123_31-26 as a GFP
379 reporter (59). The images were captured using a custom Macroscope. The detector was a Canon
380 EOS 600D Rebel T3i equipped with a Canon EFS 60mm Macro lens. GFP was excited with an
381 LED using a 470/40 filter and collected with a 480/30 filter. Remote control of the camera and
382 LED was achieved using custom software.

383

384 **Microtiter plate biofilm assays.** The ability of the rhizosphere community to form a
385 biofilm was estimated in 96-well polystyrene microtiter plates as described previously (60) with
386 some modification. Briefly, strains were grown at 28°C for 20 h; cultures were centrifuged (6000
387 × *g*, 6 min) and resuspended in sterile 10 mM NaCl to an optical density (OD) of 0.004 for
388 *Pseudomonas* spp. and 0.001 for the other isolates. Cell suspensions were placed in sterile flat-
389 bottomed microtiter plates as single species, pairs, or triple species in root exudate. Plates are
390 covered with sterile breathable sealing film and incubated at 20°C. Cell density was determined
391 by spectrophotometric measurement at 600 nm at the final time point (BioTek Synergy HT).
392 Planktonic cells were discarded, and wells were washed three times with water. Biofilms
393 attached to the wells were stained with crystal violet 0.1%, washed three times with water, and
394 dried. The stain was dissolved with 33% acetic acid, and its concentration was determined
395 spectrophotometrically at 595 nm. Visualization and statistical analyses were performed with
396 GraphPadPrism 7 software. Differences between groups were tested for statistical significance
397 (Student's t-test). Significance levels were set to * $P < 0.01$.

398

399

400 **REFERENCES**

- 401 1. **Franzosa EA, Hsu T, Sirota-Madi A, Shafquat A, Abu-Ali G, Morgan XC,**
402 **Huttenhower C.** 2015. Sequencing and beyond: integrating molecular “omics” for
403 microbial community profiling. *Nat Rev Microbiol* **13**:360–372.
- 404 2. **Oldroyd GED, Murray JD, Poole PS, Downie JA.** 2011. The rules of engagement in the
405 legume-rhizobial symbiosis. *Annu Rev Genet* **45**:119–144.
- 406 3. **Nyholm SV, McFall-Ngai MJ.** 2004. The winnowing: establishing the squid-vibrio
407 symbiosis. *Nat Rev Microbiol* **2**:632–642.
- 408 4. **Broderick NA, Lemaitre B.** 2012. Gut-associated microbes of *Drosophila melanogaster*.
409 *Gut Microbes* **3**:307–321.
- 410 5. **Buchon N, Broderick NA, Lemaitre B.** 2013. Gut homeostasis in a microbial world:
411 insights from *Drosophila melanogaster*. *Nat Rev Microbiol* **11**:615–626.
- 412 6. **Graf J.** 2016. Lessons from digestive-tract symbioses between bacteria and invertebrates.
413 *Annu Rev Microbiol* **70**:375–393.
- 414 7. **De Roy K, Marzorati M, Van den Abbeele P, Van de Wiele T, Boon N.** 2013.
415 Synthetic microbial ecosystems: an exciting tool to understand and apply microbial
416 communities. *Environ Microbiol* **16**:1472–1481.
- 417 8. **Little AEF, Robinson CJ, Peterson SB, Raffa KF, Handelsman J.** 2008. Rules of
418 engagement: interspecies interactions that regulate microbial communities. *Annu Rev*
419 *Microbiol* **62**:375–401.
- 420 9. **Shade A, Peter H, Allison SD, Baho DL, Berga M, Bürgmann H, Huber DH,**
421 **Langenheder S, Lennon JT, Martiny JBH, Matulich KL, Schmidt TM, Handelsman**
422 **J.** 2012. Fundamentals of microbial community resistance and resilience. *Front Microbiol*

- 423 **3**:417.
- 424 10. **Sánchez B, Delgado S, Blanco-Míguez A, Lourenço A, Gueimonde M, Margolles A.**
425 2017. Probiotics, gut microbiota, and their influence on host health and disease. *Mol Nutr*
426 *Food Res* **61**:1600240.
- 427 11. **Schlatter D, Kinkel L, Thomashow L, Weller D, Paulitz T.** 2017. Disease suppressive
428 soils: new insights from the soil microbiome. *Phytopathology* **107**:1284–1297.
- 429 12. **Newman DK, Banfield JF.** 2002. Geomicrobiology: how molecular-scale interactions
430 underpin biogeochemical systems. *Science* **296**:1071–1077.
- 431 13. **Fischer CN, Trautman EP, Crawford JM, Stabb EV, Handelsman J, Broderick NA.**
432 2017. Metabolite exchange between microbiome members produces compounds that
433 influence *Drosophila* behavior. *eLife* **6**:213.
- 434 14. **Madsen JS, Sørensen SJ, Burmølle M.** 2018. Bacterial social interactions and the
435 emergence of community-intrinsic properties. *Curr Opin Microbiol* **42**:104–109.
- 436 15. **Zhalnina K, Zengler K, Newman D, Northen TR.** 2018. Need for laboratory
437 ecosystems to unravel the structures and functions of soil microbial communities mediated
438 by chemistry. *mBio* **9**:805.
- 439 16. **Pessotti RC, Hansen BL, Traxler MF.** 2018. In search of model ecological systems for
440 understanding specialized Metabolism. *mSystems* **3**:457.
- 441 17. **Wolfe BE.** 2018. Using cultivated microbial communities to dissect microbiome
442 assembly: challenges, limitations, and the path ahead. *mSystems* **3**:1211.
- 443 18. **Venturelli OS, Carr AC, Fisher G, Hsu RH, Lau R, Bowen BP, Hromada S, Northen**
444 **T, Arkin AP.** 2018. Deciphering microbial interactions in synthetic human gut
445 microbiome communities. *Mol Syst Biol* **14**:e8157.

- 446 19. **Wolfe BE, Button JE, Santarelli M, Dutton RJ.** 2014. Cheese rind communities provide
447 tractable systems for in situ and in vitro studies of microbial diversity. *Cell* **158**:422–433.
- 448 20. **Niu B, Paulson JN, Zheng X, Kolter R.** 2017. Simplified and representative bacterial
449 community of maize roots. *Proc Natl Acad Sci USA* **114**:E2450–E2459.
- 450 21. **Lozano GL, Bravo JI, Handelsman J.** 2017. Draft genome sequence of *Pseudomonas*
451 *koreensis* CI12, a *Bacillus cereus* “hitchhiker” from the soybean rhizosphere. *Genome*
452 *Announc* **5**:e00570–17.
- 453 22. **Peterson SB, Dunn AK, Klimowicz AK, Handelsman J.** 2006. Peptidoglycan from
454 *Bacillus cereus* mediates commensalism with rhizosphere bacteria from the *Cytophaga-*
455 *Flavobacterium* group. *Appl Environ Microbiol* **72**:5421–5427.
- 456 23. **Barton NH.** 2000. Genetic hitchhiking. *Philos Trans R Soc Lond, B, Biol Sci* **355**:1553–
457 1562.
- 458 24. **Bulgarelli D, Schlaeppi K, Spaepen S, Ver Loren van Themaat E, Schulze-Lefert P.**
459 2013. Structure and functions of the bacterial microbiota of plants. *Annu Rev Plant Biol*
460 **64**:807–838.
- 461 25. **Foster KR, Bell T.** 2012. Competition, not cooperation, dominates interactions among
462 culturable microbial species. *Curr Biol* **22**:1845–1850.
- 463 26. **Vetsigian K, Jajoo R, Kishony R.** 2011. Structure and evolution of *Streptomyces*
464 interaction networks in soil and in silico. *PLoS Biol* **9**:e1001184.
- 465 27. **Dunne JA, Williams RJ, Martinez ND.** 2002. Food-web structure and network theory:
466 the role of connectance and size. *Proc Natl Acad Sci USA* **99**:12917–12922.
- 467 28. **Weller DM.** 2007. *Pseudomonas* biocontrol agents of soilborne pathogens: looking back
468 over 30 years. *Phytopathology* **97**:250–256.

- 469 29. **Stragier P, Losick R.** 1996. Molecular genetics of sporulation in *Bacillus subtilis*. *Annu*
470 *Rev Genet* **30**:297–241.
- 471 30. **Lozano GL, Park HB, Bravo JI, Armstrong EA, Denu JM, Stabb EV, Broderick NA,**
472 **Crawford JM, Handelsman J.** 2018. Bacterial analogs of plant piperidine alkaloids
473 mediate microbial interactions in a rhizosphere model system. bioRxiv 499731.
- 474 31. **Vilain S, Luo Y, Hildreth MB, Brozel VS.** 2006. Analysis of the life cycle of the soil
475 saprophyte *Bacillus cereus* in liquid soil extract and in soil. *Appl Environ Microbiol*
476 **72**:4970–4977.
- 477 32. **Stabb EV, Jacobson LM, Handelsman J.** 1994. Zwittermicin A-producing strains of
478 *Bacillus cereus* from diverse soils. *Appl Environ Microbiol* **60**:4404–4412.
- 479 33. **Halverson LJ, Handelsman J.** 1991. Enhancement of soybean nodulation by *Bacillus*
480 *cereus* UW85 in the field and in a growth chamber. *Appl Environ Microbiol* **57**:2767–
481 2770.
- 482 34. **Gilbert G, Clayton M, Handelsman J, Parke J.** 1996. Use of cluster and discriminant
483 analyses to compare rhizosphere bacterial communities following biological perturbation.
484 *Microb Ecol* **32**:123–147.
- 485 35. **Osburn RM, Milner JL, Oplinger ES, Smith RS, Handelsman J.** 1995. Effect of
486 *Bacillus cereus* UW85 on the yield of soybean at two field sites in Wisconsin. *Plant*
487 *Disease* **79**:551.
- 488 36. **Bullied WJ, Buss TJ, Kevin Vessey J.** 2002. *Bacillus cereus* UW85 inoculation effects
489 on growth, nodulation, and N accumulation in grain legumes: field studies. *Canadian J*
490 *Plant Sci* **82**:291–298.
- 491 37. **Lozano GL, Holt J, Ravel J, Rasko DA, Thomas MG, Handelsman J.** 2016. Draft

- 492 genome sequence of biocontrol agent *Bacillus cereus* UW85. *Genome Announc*
493 4:e00910–16.
- 494 38. **Bravo JI, Lozano GL, Handelsman J.** 2017. Draft genome sequence of *Flavobacterium*
495 *johnsoniae* CI04, an isolate from the soybean rhizosphere. *Genome Announc* 5:e01535–
496 16.
- 497 39. **Delgado-Baquerizo M, Oliverio AM, Brewer TE, Benavent-González A, Eldridge DJ,**
498 **Bardgett RD, Maestre FT, Singh BK, Fierer N.** 2018. A global atlas of the dominant
499 bacteria found in soil. *Science* 359:320–325.
- 500 40. **Rascovan N, Carbonetto B, Perrig D, Díaz M, Canciani W, Abalo M, Alloati J,**
501 **González-Anta G, Vazquez MP.** 2016. Integrated analysis of root microbiomes of
502 soybean and wheat from agricultural fields. *Sci Rep* 6:28084.
- 503 41. **Rahman KSM, Thahira-Rahman J, Lakshmanaperumalsamy P, Banat IM.** 2002.
504 Towards efficient crude oil degradation by a mixed bacterial consortium. *Bioresour*
505 *Technol* 85:257–261.
- 506 42. **Gangwar P, Alam SI, Singh L.** 2011. Metabolic characterization of cold active
507 *Pseudomonas*, *Arthrobacter*, *Bacillus*, and *Flavobacterium* spp. from Western Himalayas.
508 *Indian J Microbiol*, 2nd ed. 51:70–75.
- 509 43. **König H.** 2006. *Bacillus* species in the intestine of termites and other soil invertebrates. *J*
510 *Appl Microbiol* 101:620–627.
- 511 44. **Warwick C, Arena PC, Steedman C.** 2013. Health implications associated with
512 exposure to farmed and wild sea turtles. *JRSM Short Rep* 4:8–7.
- 513 45. **Liu Y, Kyle S, Straight PD.** 2018. Antibiotic stimulation of a *Bacillus subtilis* migratory
514 response. *mSphere* 3:e00586–17.

- 515 46. **McCully LM, Bitzer AS, Seaton SC, Smith LM, Silby MW.** 2018. Social motility:
516 interaction between two sessile soil bacteria leads to emergence of surface motility.
517 bioRxiv 296814.
- 518 47. **Hsueh YH, Somers EB, Lereclus D, Ghelardi E, Wong ACL.** 2007. Biosurfactant
519 production and surface translocation are regulated by PlcR in *Bacillus cereus* ATCC
520 14579 under low-nutrient conditions. *Appl Environ Microbiol* **73**:7225–7231.
- 521 48. **Hölscher T, Kovács ÁT.** 2017. Sliding on the surface: bacterial spreading without an
522 active motor. *Environ Microbiol* **19**:2537–2545.
- 523 49. **Danhorn T, Fuqua C.** 2007. Biofilm formation by plant-associated bacteria. *Annu Rev*
524 *Microbiol* **61**:401–422.
- 525 50. **Kelsic ED, Zhao J, Vetsigian K, Kishony R.** 2015. Counteraction of antibiotic
526 production and degradation stabilizes microbial communities. *Nature* **521**:516–519.
- 527 51. **Narisawa N, Haruta S, Arai H, Ishii M, Igarashi Y.** 2008. Coexistence of antibiotic-
528 producing and antibiotic-sensitive bacteria in biofilms is mediated by resistant bacteria.
529 *Appl Environ Microbiol* **74**:3887–3894.
- 530 52. **Friedman J, Higgins LM, Gore J.** 2017. Community structure follows simple assembly
531 rules in microbial microcosms. *Nat Ecol Evol* **1**:109.
- 532 53. **Pérez-Gutiérrez R-A, López-Ramírez V, Islas Á, Alcaraz LD, Hernández-González I,**
533 **Olivera BCL, Santillán M, Eguiarte LE, Souza V, Trivisano M, Olmedo-Alvarez G.**
534 2013. Antagonism influences assembly of a *Bacillus* guild in a local community and is
535 depicted as a food-chain network. *ISME J* **7**:487–497.
- 536 54. **Wright ES, Vetsigian KH.** 2016. Inhibitory interactions promote frequent bistability
537 among competing bacteria. *Nat Commun* **7**:11274.

- 538 55. **Handelsman J.** 2009. Metagenetics: spending our inheritance on the future. *Microb*
539 *Biotechnol* **2**:138–139.
- 540 56. **Hoagland DR, Arnon DI.** 1950. The water-culture method for growing plants without
541 soil. *Calif Agric Exp Stat Circ* **347**:1–32.
- 542 57. **Shannon P, Markiel A, Ozier O, Baliga NS, Wang JT, Ramage D, Amin N,**
543 **Schwikowski B, Ideker T.** 2003. Cytoscape: a software environment for integrated
544 models of biomolecular interaction networks. *Genome Res* **13**:2498–2504.
- 545 58. **Klimowicz AK, Benson TA, Handelsman J.** 2010. A quadruple-enterotoxin-deficient
546 mutant of *Bacillus thuringiensis* remains insecticidal. *Microbiology* **156**:3575–3583.
- 547 59. **Dunn AK, Handelsman J.** 1999. A vector for promoter trapping in *Bacillus cereus*. *Gene*
548 **226**:297–305.
- 549 60. **Wijman JGE, de Leeuw PPLA, Moezelaar R, Zwietering MH, Abee T.** 2007. Air-
550 liquid interface biofilms of *Bacillus cereus*: formation, sporulation, and dispersion. *Appl*
551 *Environ Microbiol* **73**:1481–1488.

552

553

554 **FIGURES AND TABLES**

555

556 **FIG 1.** Network analysis of inhibitory interactions among rhizosphere isolates. (A) Venn
557 diagram of the inhibitory interactions in isolates in three media: Luria-Bertani agar (LBA), 1/2-
558 strength tryptic soy agar (TSA) and 1/10th-strength TSA. (B) Colors indicate phylogeny of
559 isolates used in the inhibitory matrix and network. (C) Inhibitory interaction matrix between *B.*
560 *cereus* UW85 and hitchhiker isolates in three media. Potential producers, which are isolates
561 tested for the ability to inhibit others, are on the y-axis and receivers, which are isolates tested for
562 inhibition by others, are on the x-axis. There are two different color codes used in (C). One
563 indicates the phylogeny of isolates in the row and column title, and second one for the matrix
564 results using the colors scheme shown in the Venn diagram corresponding to the medium in
565 which the interaction appears. (D) Hierarchy scoring scheme used to organize the isolates in the
566 hierarchy interaction network, in which black is the focal point. (E-F) Inhibitory interaction
567 network organized by hierarchy score. (E) Inhibitory interactions generated from the isolates
568 with high hierarchy scores. (F) Inhibitory interactions generated from the isolates with medium
569 and low hierarchy scores. (G) Reciprocal inhibitory interactions observed in the inhibitory
570 network. Orange indicates interactions observed in only 1 medium, and black indicates
571 interactions observed in 2 or 3 media.

572

573 **FIG 2.** Co-culture of rhizosphere isolates with *Pseudomonas spp.* and *B. cereus* UW85. (A)
574 Competition experiments between *F. johnsoniae* CI04 and either *Pseudomonas sp.* CI14,
575 *Pseudomonas sp.* RI46, or *P. koreensis* CI12, in three media: Luria-Bertani broth (LB), 1/2-
576 strength tryptic soy broth (TSB) and soybean root exudate. (B) Rhizosphere isolates were grown

577 alone or in co-culture with *P. koreensis* CI12 in soybean root exudate. Colored bars under x-axis
578 indicate phylogenetic groups as in Fig. 1. (C) *F. johnsoniae* CI04 grown alone, in co-culture with
579 *P. koreensis* CI12 or *B. cereus* UW85, and in triple culture with *P. koreensis* CI12 and *B. cereus*
580 UW85. Gray dotted line, limit of detection.

581
582 **FIG 3.** Effect of *Bacillus* spp. on populations of *F. johnsoniae* in the presence of *P. koreensis*.
583 Triple culture of *P. koreensis* CI12, *F. johnsoniae* CI04, and either *B. subtilis* NCIB3160 or *B.*
584 *cereus* UW85, or their mutants. Gray dotted line, limit of detection.

585
586 **FIG 4.** *B. cereus* UW85 colony expansion in the presence of the rhizosphere isolates. (A)
587 Schematic representation of the spread-patch plates. (B) *B. cereus* UW85 grown alone. (C) *B.*
588 *cereus* UW85 grown on a lawn of each member of the community. Photographs taken after 4
589 days at 28°C. Arrows indicate the limits of the *B. cereus* colony.

590
591 **FIG 5.** Effect of community members on *B. cereus* UW85 colony expansion. (A) *B. cereus*
592 UW85 plasmid-dependent GFP strain grown alone or on a lawn of *P. koreensis* CI12, *F.*
593 *johnsoniae* CI04, or *Paenibacillus* sp. RI40. Bright-field (BF) and GFP imaging of colonies five
594 days after inoculation. (B) *B. cereus* UW85 GFP strain grown in close proximity to a colony of
595 *P. koreensis* CI12, *F. johnsoniae* CI04, or *Paenibacillus* sp. RI40. Arrows indicate *B. cereus*
596 UW85 expansion over colonies of the other isolates. Bright-field, GFP channel, and overlay of
597 the two channels of plates after 2 days growth (*F. johnsoniae* CI04) and after 5 days growth (*P.*
598 *koreensis* CI12 and *Paenibacillus* sp. RI40).

599

600 **FIG 6.** Biofilm formation by rhizosphere isolates. Biofilm was quantified by measuring the
601 OD₅₉₅ after staining with crystal violet. (A) Crystal violet quantification of biofilm formation
602 for each of the 21 isolates at 12 and 24 hours after inoculation. (B-D) *Pseudomonas* biofilm
603 production when grown with a poor biofilm producer normalized against *Pseudomonas* biofilm
604 in pure culture at 12 and 24 hours (B) *Pseudomonas* sp. RI46 (C) *Pseudomonas* sp. CI14 (D) *P.*
605 *koreensis* CI12. (E) Biofilm formation by *P. koreensis* CI12 growing alone, in co-culture with
606 either *F. johnsoniae* CI04 or *B. cereus* UW85, and in triple culture at 12, 18, 24, and 36 hours.
607 (F) *P. koreensis* CI12 biofilm production when grown with two other isolates normalized against
608 *P. koreensis* growth in pure culture. * indicates p<0.01. Colored bars under x-axis indicate
609 phylogenetic groups as in Fig. 1. Gray dotted line, limit of detection.

610

611 **TABLE 1.** Accumulation of koreenceine A, B, and C in co-culture with *F. johnsoniae* or *B.*
612 *cereus*. Koreenceine A, B, and C concentrations are expressed as ion counts from LC/HR-ESI-
613 QTOF-MS analysis from cell-free filtrates of cultures of *P. koreensis* CI12 grown alone, with *F.*
614 *johnsoniae* CI04, *F. johnsoniae* CI04 and *B. cereus* UW85 wild type, or with *F. johnsoniae* CI04
615 and *B. cereus* UW85 *spo0H*. *F. johnsoniae* CI04 population growth in the corresponding
616 conditions in CFU/mL. ND, not detected.

617

618 **FIG S1.** *P. koreensis* CI12 population dynamics. *P. koreensis* CI12 grown alone, in co-culture
619 with *F. johnsoniae* CI04 or *B. cereus* UW85, and in triple culture with *F. johnsoniae* CI04 and *B.*
620 *cereus* UW85.

621

622 **FIG S2.** Correlation between *Bacillus spp.* spore density and *F. johnsoniae* protection in triple
623 culture. Triple culture of *F. johnsoniae* CI04 and *P. koreensis* CI12 with either *B. cereus* UW85
624 (A) or *B. subtilis* NCIB3160 (B). The cell density of the *Bacillus* inoculum is on the x-axis.
625 *Bacillus* spore densities and *F. johnsoniae* CI04 cell densities in the triple culture at 30 h are on
626 the y-axis. Gray dotted line, limit of detection.

627

628 **FIG S3.** *P. koreensis* CI12 biofilm quantification and growth of the planktonic population. *P.*
629 *koreensis* CI12 growth is on the left y-axis and crystal violet quantification of biofilm formation
630 for *P. koreensis* CI12 is on the right y-axis.

631

632 **TABLE S1.** Area of *B. cereus* colonies is larger in the presence of either *F. johnsoniae* or *P.*
633 *koreensis*.

634

635 **TABLE S2.** Strains used in this study.

636

637 **TABLE S3.** Primers used in this study.

FIG 1.

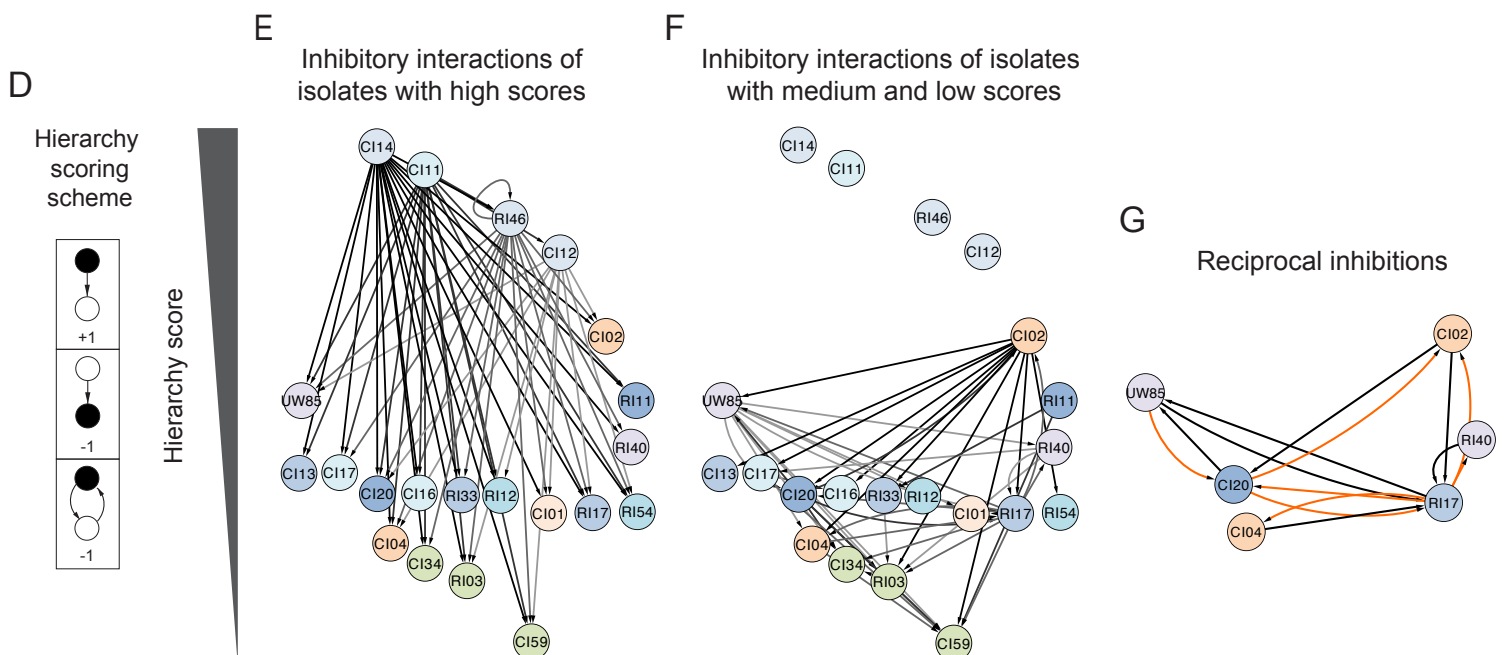
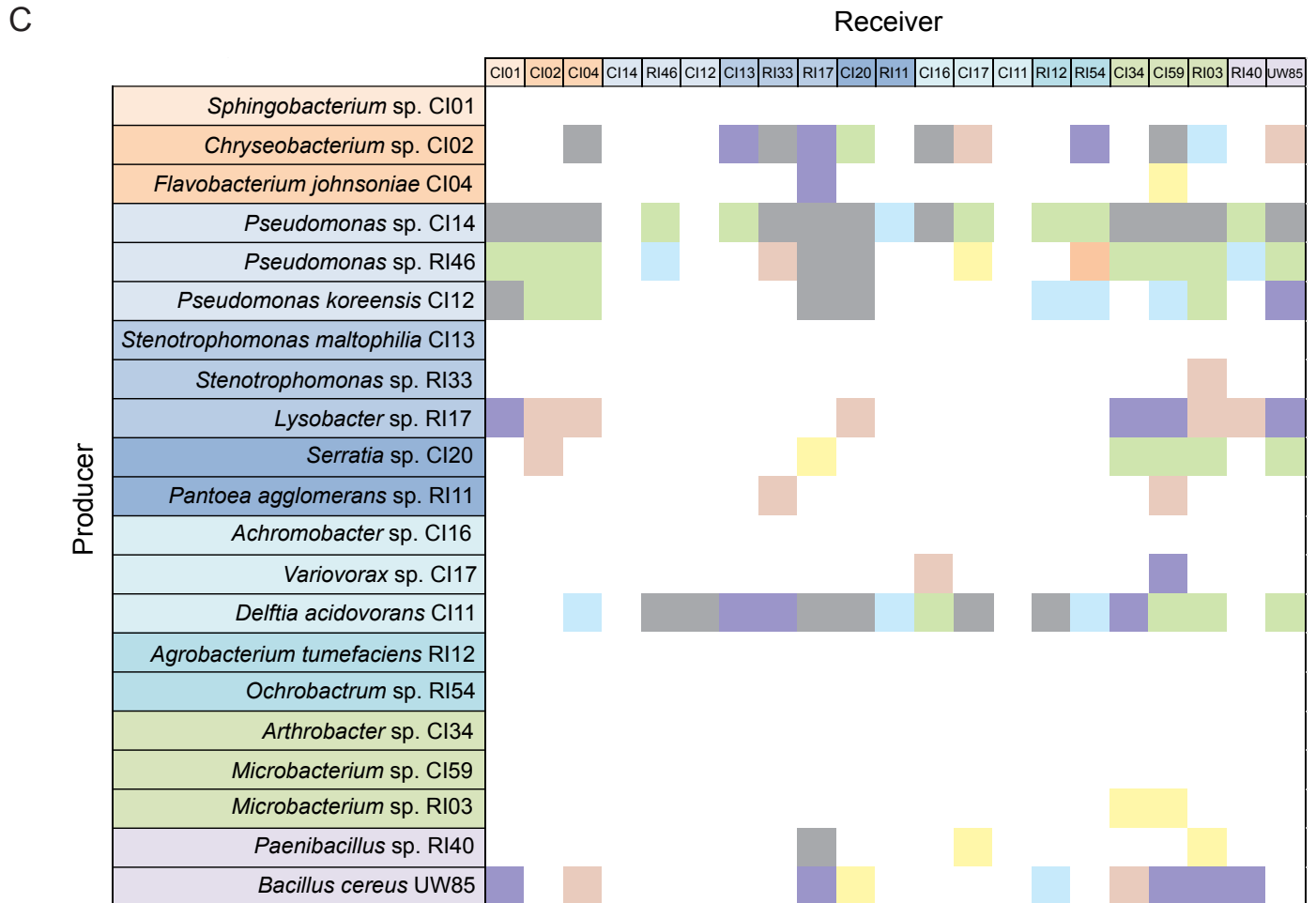
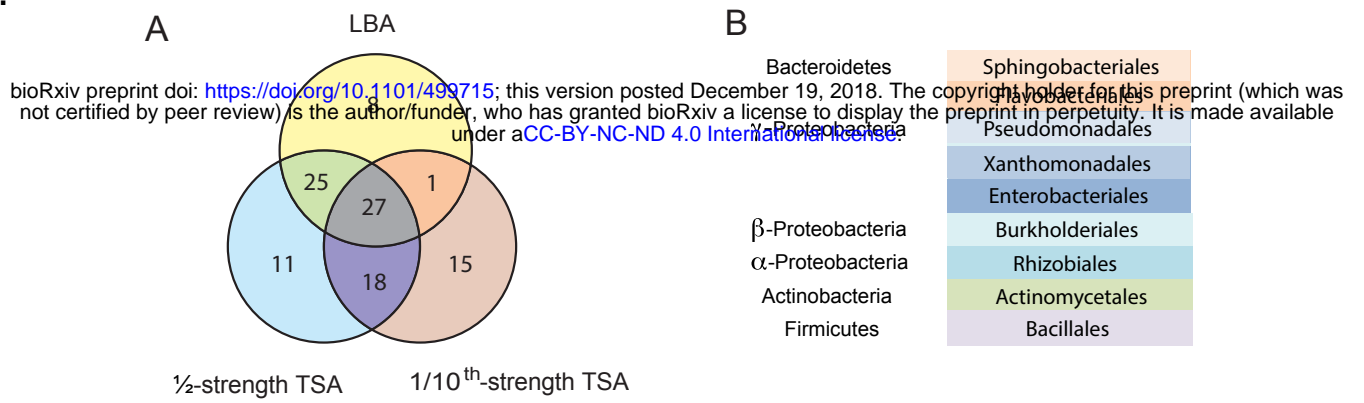


FIG 2.

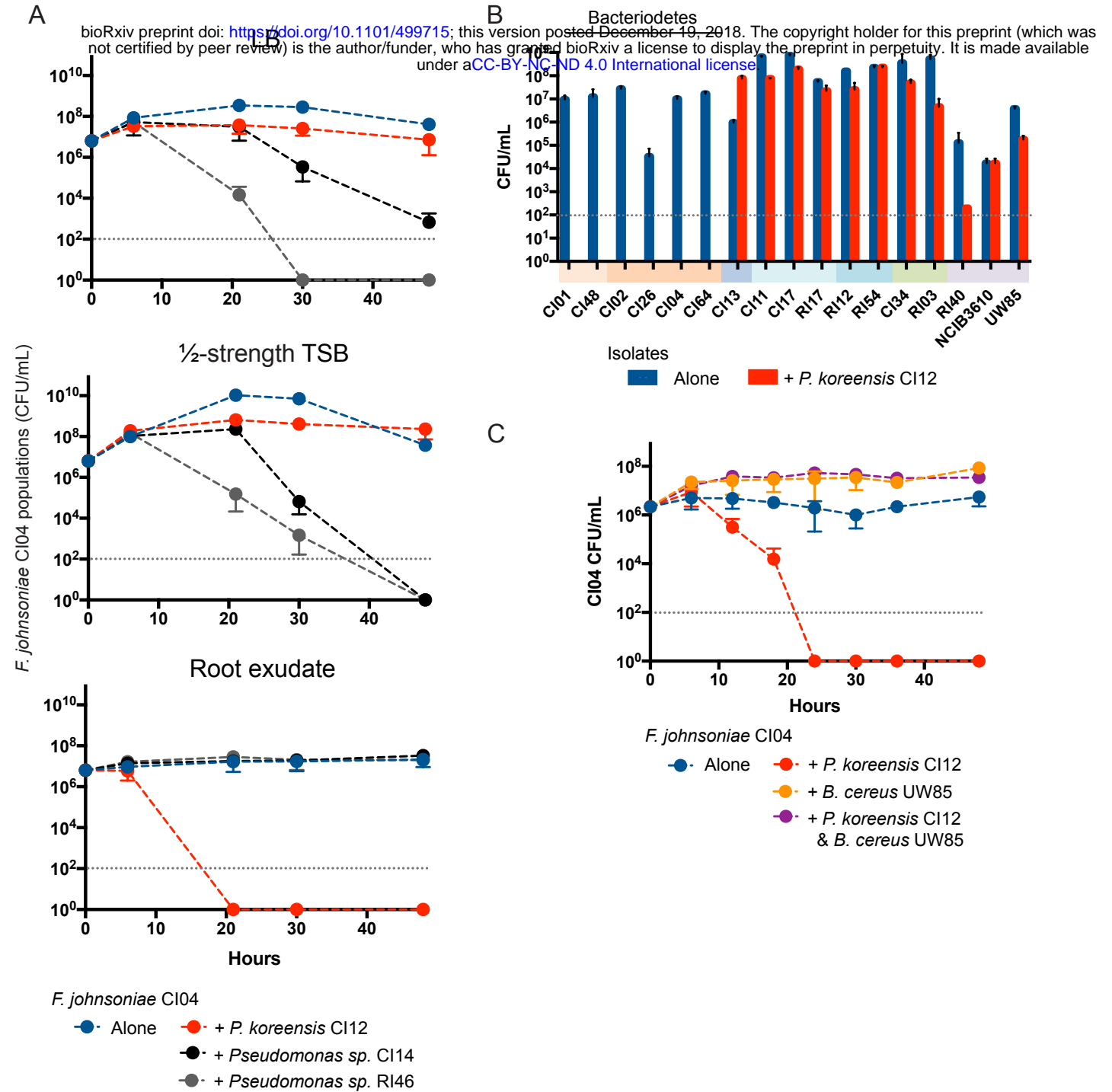


FIG 3.

bioRxiv preprint doi: <https://doi.org/10.1101/499715>; this version posted December 19, 2018. The copyright holder for this preprint (which was not certified by peer review) is the author/funder, who has granted bioRxiv a license to display the preprint in perpetuity. It is made available under aCC-BY-NC-ND 4.0 International license.

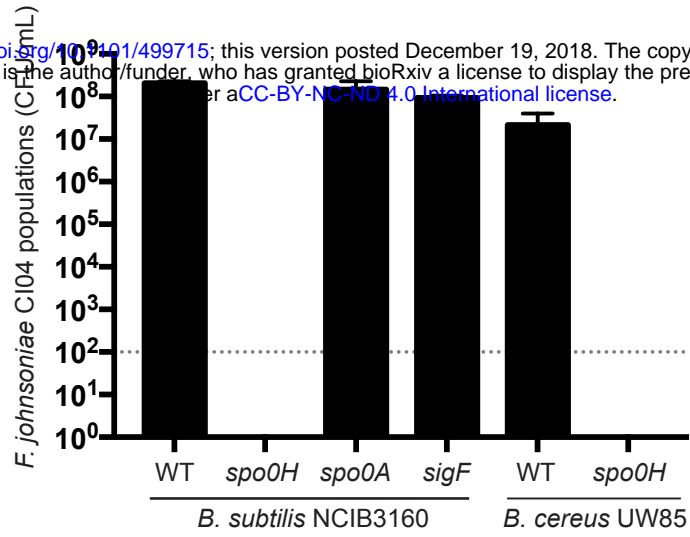


FIG 4.

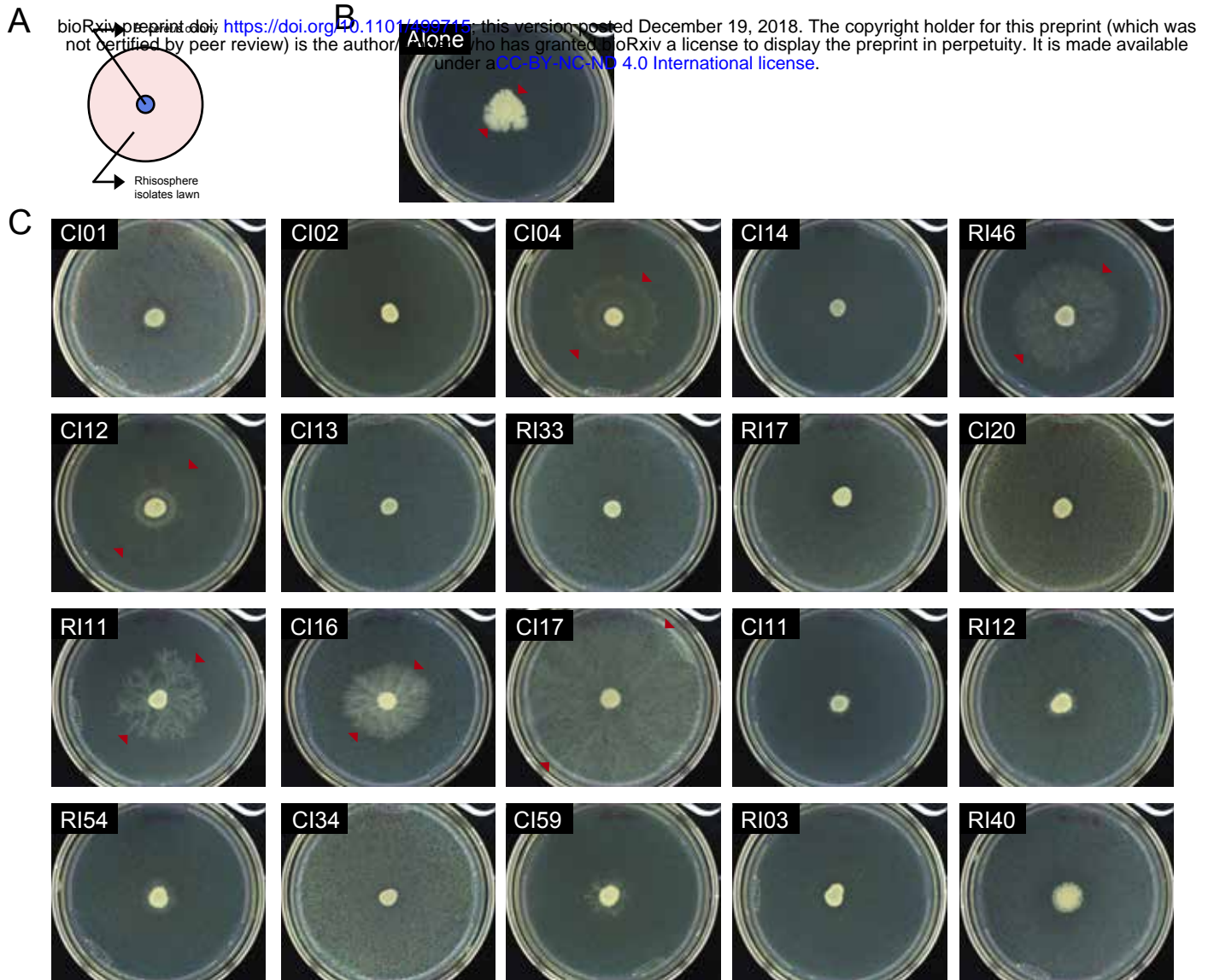
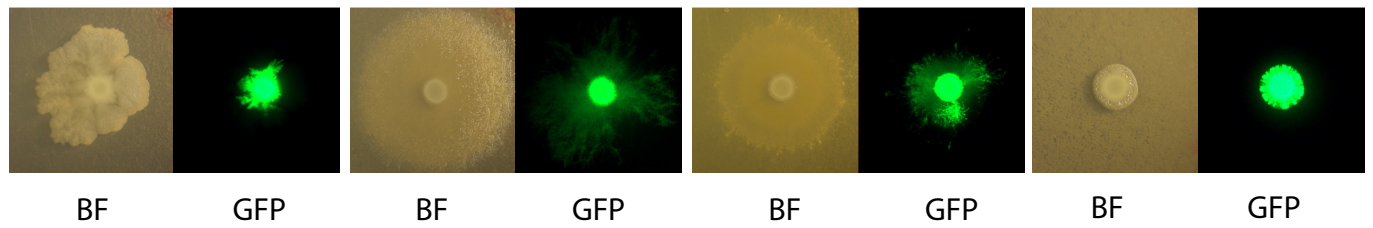


FIG 5.

A

bioRxiv preprint doi: <https://doi.org/10.1101/499715>; this version posted December 19, 2018. The copyright holder for this preprint (which was not certified by peer review) is the author/funder, who has granted bioRxiv a license to display the preprint in perpetuity. It is made available under aCC-BY-NC-ND 4.0 International license.



B

B. cereus UW85
+ *P. koreensis* CI12

+ *F. johnsoniae* CI04

+ *Paenibacillus* sp. RI40

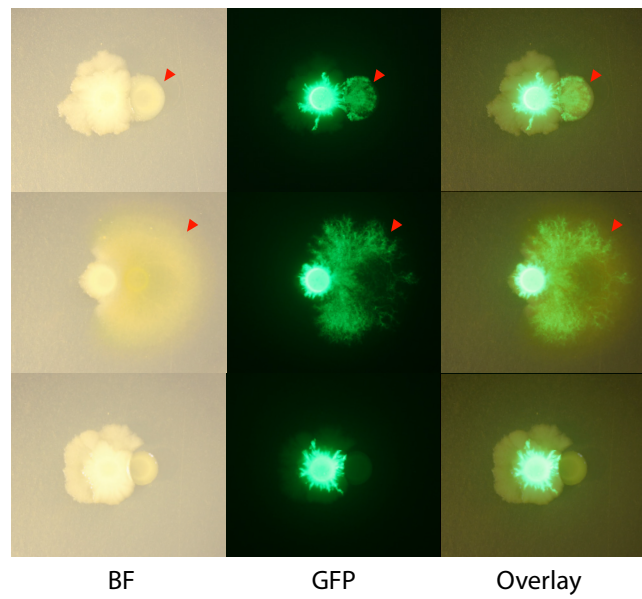
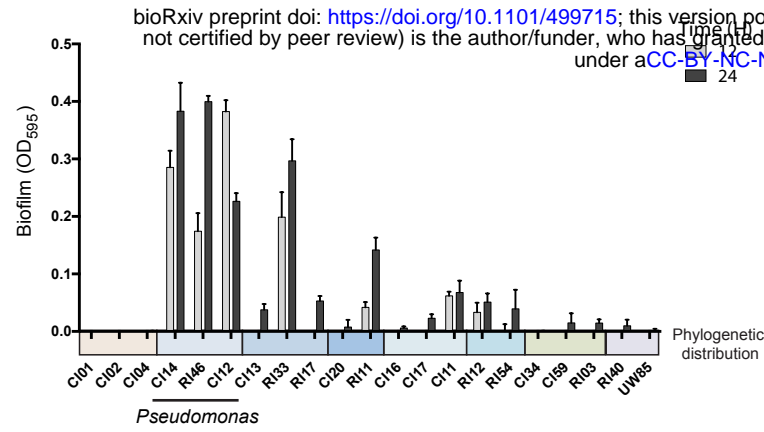
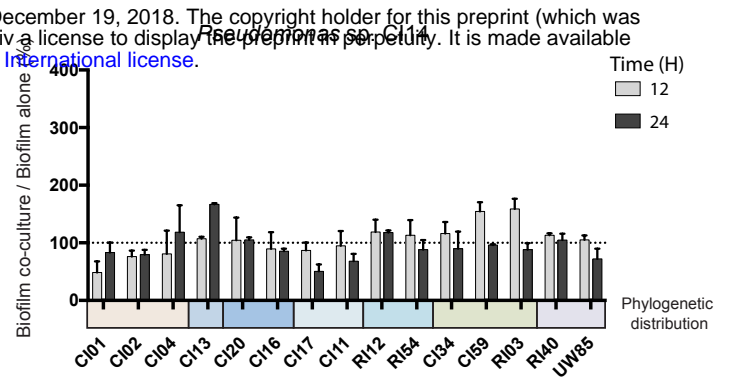


FIG 6.

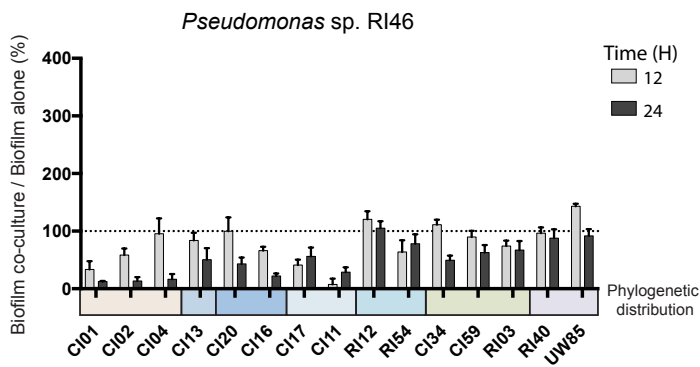
A



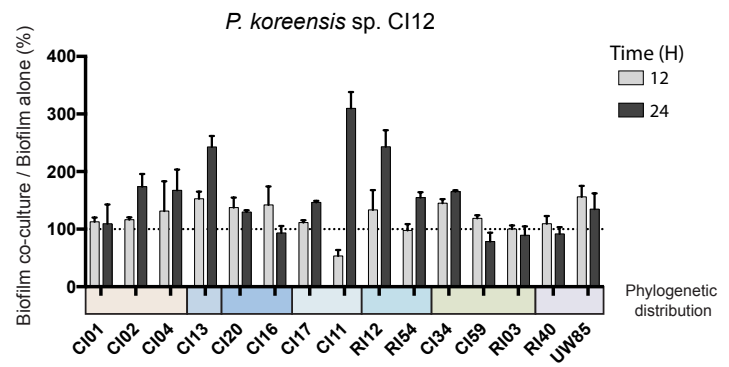
B



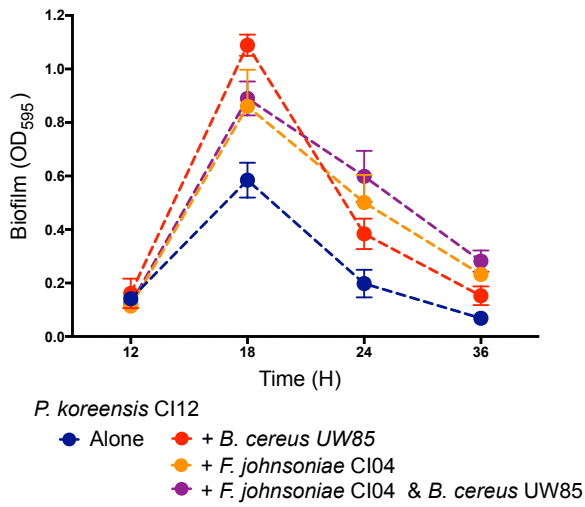
C



D



E



F

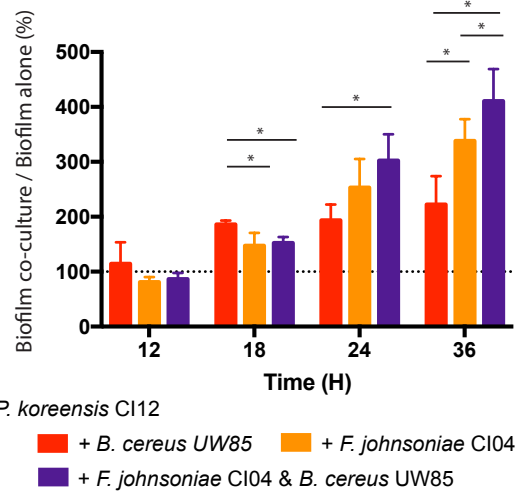


TABLE 1.

bioRxiv preprint doi: <https://doi.org/10.1101/499715>; this version posted December 19, 2018. The copyright holder for this preprint (which was not certified by peer review) is the author/funder, who has granted bioRxiv a license to display the preprint in perpetuity. It is made available under aCC-BY-NC-ND 4.0 International license.

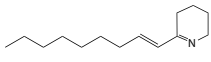
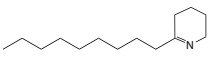
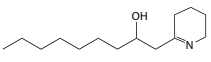
Source of cell-free extracts	<i>F. johnsoniae</i> growth (10 ⁷ CFU/mL)	Accumulation of koreenceine A, B and C (relative ion counts x10 ⁵)		
		Koreenceine A 	Koreenceine B 	Koreenceine C 
<i>P. koreensis</i>	1.4 ± 0.4	3.6 ± 0.4	62.9 ± 5.5	3.2 ± 0.4
<i>P. koreensis</i> with <i>F. johnsoniae</i>	ND	75.9 ± 11.4	275.9 ± 17.9	35.3 ± 6.5
<i>P. koreensis</i> with <i>F. johnsoniae</i> and <i>B. cereus</i> WT	6.3 ± 1.2	3.1 ± 0.4	167.6 ± 17.3	0.7 ± 0.2
<i>P. koreensis</i> with <i>F. johnsoniae</i> and <i>B. cereus spo0H</i>	ND	31.5 ± 9.8	310.1 ± 54.1	7.4 ± 2.6

FIG S1.

bioRxiv preprint doi: <https://doi.org/10.1101/499715>; this version posted December 19, 2018. The copyright holder for this preprint (which was not certified by peer review) is the author/funder, who has granted bioRxiv a license to display the preprint in perpetuity. It is made available under aCC-BY-NC-ND 4.0 International license.

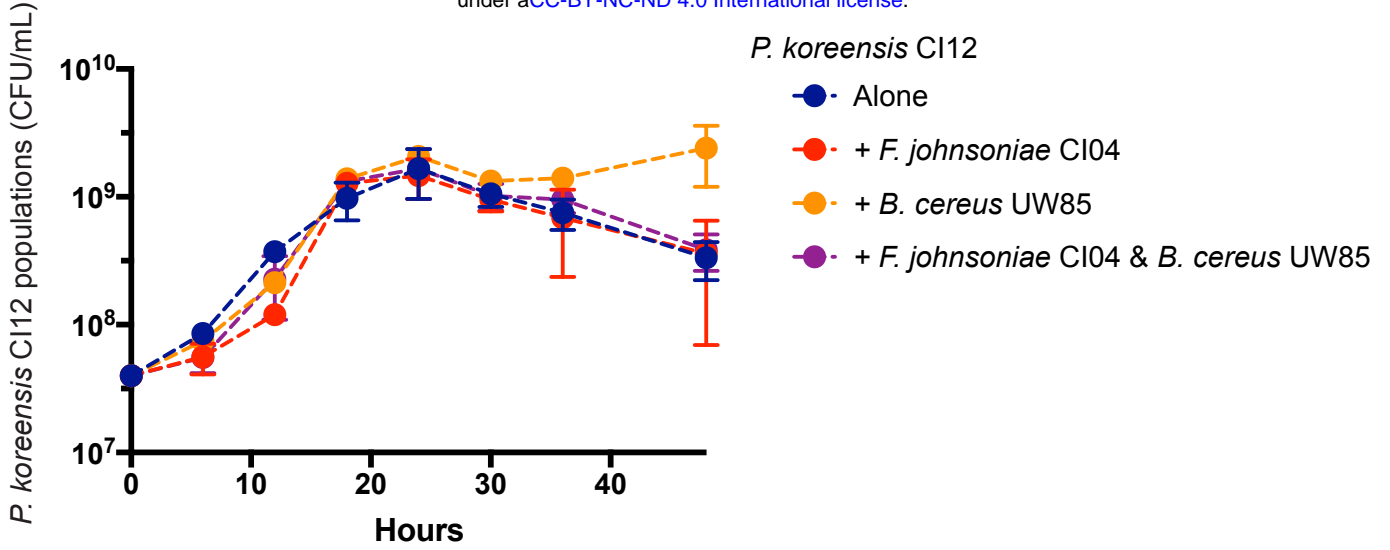


FIG S2.

bioRxiv preprint doi: <https://doi.org/10.1101/499715>; this version posted December 19, 2018. The copyright holder for this preprint (which was not certified by peer review) is the author/funder, who has granted bioRxiv a license to display the preprint in perpetuity. It is made available under aCC-BY-NC-ND 4.0 International license.

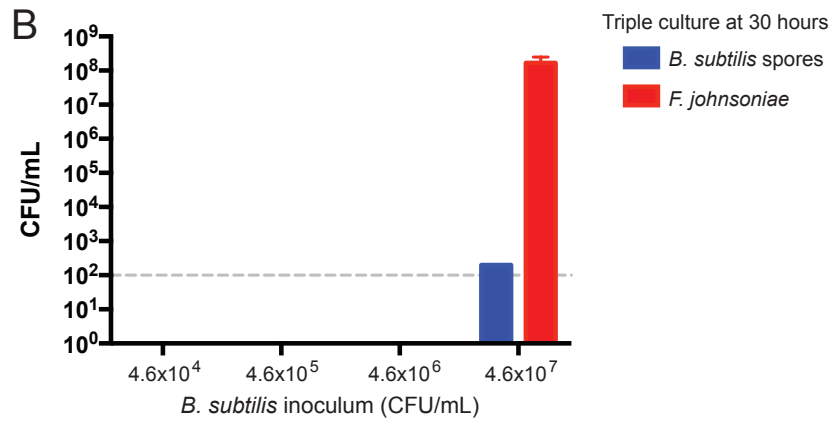
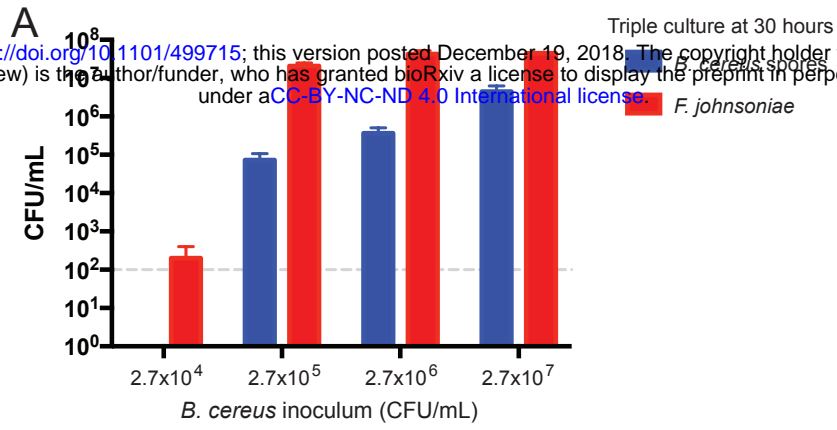


FIG S3.

bioRxiv preprint doi: <https://doi.org/10.1101/499715>; this version posted December 19, 2018. The copyright holder for this preprint (which was not certified by peer review) is the author/funder, who has granted bioRxiv a license to display the preprint in perpetuity. It is made available under aCC-BY-NC-ND 4.0 International license.

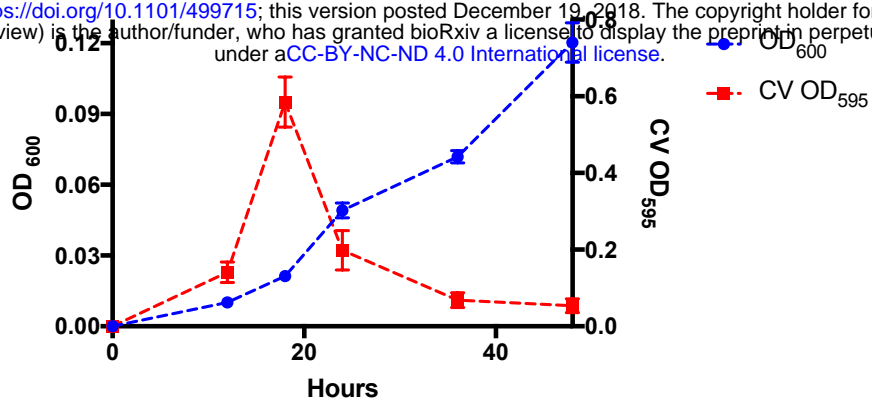


TABLE S1.

	Area <i>B. cereus</i> colony (cm ²)	
	Day 2	Day 5
<i>B. cereus</i> alone	1.3 +- 0.06	6.3 +- 0.42
<i>B. cereus</i> with <i>F. johnsoniae</i>	3.0 +- 0.24	24.3 +- 0.55
<i>B. cereus</i> with <i>P. koreensis</i>	1.8 +- 0.2	23.8 +- 2.66

TABLE S2.

Name	Phyla	Family	Abbreviation
<i>Sphingobacterium</i> sp. CI01	Bacteroidetes	Sphingobacteriales	CI01
<i>Chryseobacterium</i> sp. CI02	Bacteroidetes	Flavobacteriales	CI02
<i>Flavobacterium johnsoniae</i> CI04	Bacteroidetes	Flavobacteriales	CI04
<i>Pseudomonas</i> sp. CI14	Proteobacteria	Pseudomonadales	CI14
<i>Pseudomonas</i> sp. RI46	Proteobacteria	Pseudomonadales	RI46
<i>Pseudomonas koreensis</i> CI12	Proteobacteria	Pseudomonadales	CI12
<i>Stenotrophomonas maltophilia</i> CI13	Proteobacteria	Xanthomonadales	CI13
<i>Lysobacter</i> sp. RI17	Proteobacteria	Xanthomonadales	RI17
<i>Serratia</i> sp. CI20	Proteobacteria	Enterobacteriales	CI20
<i>Pantoea agglomerans</i> sp. RI11	Proteobacteria	Enterobacteriales	RI11
<i>Achromobacter</i> sp. CI16	Proteobacteria	Burkholderiales	CI16
<i>Variovorax</i> sp. CI17	Proteobacteria	Burkholderiales	CI17
<i>Stenotrophomonas maltophilia</i> RI33	Proteobacteria	Burkholderiales	RI33
<i>Delftia acidovorans</i> CI11	Proteobacteria	Burkholderiales	CI11
<i>Agrobacterium tumefaciens</i> RI12	Proteobacteria	Rhizobiales	RI12
<i>Ochrobactrum</i> sp. RI54	Proteobacteria	Rhizobiales	RI54
<i>Arthrobacter</i> sp. CI34	Actinobacteria	Actinomycetales	CI34
<i>Microbacterium</i> sp. CI59	Actinobacteria	Actinomycetales	CI59
<i>Microbacterium</i> sp. RI03	Actinobacteria	Actinomycetales	RI03
<i>Paenibacillus</i> sp. RI40	Firmicutes	Bacillales	RI40
<i>Bacillus cereus</i> UW85	Firmicutes	Bacillales	UW85
<i>Sphingobacterium</i> sp. CI48	Bacteroidetes	Sphingobacteriales	CI48
<i>Chryseobacterium</i> sp. CI26	Bacteroidetes	Flavobacteriales	CI26
<i>Flavobacterium johnsoniae</i> CI64	Bacteroidetes	Flavobacteriales	CI64
<i>Bacillus subtilis</i> NCIB3160	Firmicutes	Bacillales	NCIB3160

TABLE S3.

Name	Sequence
mut_spo0HA1	CACCGGATCCGCCAATTGGGTTAGTAATTGGTAGTGAAGG
mut_spo0HA2	GACAATGTCAATGACATGCATTTTGTACTGTCC TTGATCCCTCCGACCGCTATTTATTAG
mut_spo0HB1	CTAAATAAATAGCGGTCGGAGGGATCAAGGACAGTACAAAATGCATGTCATTGACATTGTC
mut_spo0HB2	GGATCCACGTACAACATACCAAGAATCATCAGTCATG